International Journal of Applied Glass Science 3 [4] 321–331 (2012)
DOI:10.1111/ijag.12006

INTERNATIONAL JOURNAL OF
Applied Glass
SCIENCE

Study of Lanthanum Aluminum Silicate Glasses for Passive and Active Optical Fibers

Doris Litzkendorf,* Stephan Grimm, Kay Schuster, Jens Kobelke, Anka Schwuchow, Anne Ludwig, Johannes Kirchhof, Martin Leich, Sylvia Jetschke, and Jan Dellith

Institute of Photonic Technology, Department of Fiber Optics, Jena, 07745, Germany

Jean-Louis Auguste and Georges Humbert

Institute de recherche Xlim, UMR CNRS 7252, Limoges, 87060, France

We are reporting on SiO_2-Al_2O_3-La_2O_3 glasses—with and without Yb_2O_3—suitable for nonlinear and fiber laser applications. We will also be presenting successful supercontinuum generation and fiber laser operation around 1060 nm in step-index fibers. We optimized the glass compositions in terms of thermal and optical requirements for both a high La_2O_3 and Yb_2O_3 concentration and good compatibility with a silica cladding. We also produced bulk samples, unstructured fibers, and structured fibers with a SiO_2-Al_2O_3-La_2O_3 core and silica cladding for this purpose.

Introduction

Optical fibers with improved properties can be achieved using new core glass materials. In recent years, the advantages of multicomponent oxide glasses (MCGs) based on lanthanum aluminum silicate have been recognized for different fiber applications, such as high nonlinear fibers for supercontinuum generation, optical fiber switching, or Raman amplifiers/lasers and fibers with very high rare earth (RE) concentration for fiber lasers and amplifiers.

*doris.litzkendorf@ipht-jena.de

Fibers used for nonlinear applications (passive fibers) must have certain properties, such as high optical nonlinearity and an optimized chromatic dispersion. The nonlinear effect depends on the nonlinear parameter γ

$$\gamma = \frac{2 \cdot \pi \cdot n_2}{\lambda \cdot A}$$

where n_2 is the nonlinear refractive index of the glass, λ is the operating wavelength, and A is the effective area of the light propagating core. Thus, the nonlinearity of optical fibers can be influenced by tuned glass materials (e.g., nonsilica glasses), fiber microstructuring,

or both.[1–7] However, silica fibers show a nonlinear coefficient of only $n_2 = 2.4*10^{-20}$ m^2/W.[8] Various oxide glasses, lead silicates, bismuth silicates, tellurites, bismuth borates, and antimony oxide glasses[9,10] have been studied in the past regarding their suitability for nonlinear fiber applications due to their large amounts of highly polarizable heavy metal ions. Supercontinuum generation was successfully demonstrated in fibers made from different multicomponent oxide glasses.[11–15] Furthermore, these materials often show an expanded operation wavelength range for nonlinear conversion processes.

RE-doped fibers (active fibers) are commonly used for laser operation in continuous or pulsed mode. The materials providing the basis for these fibers should show low nonlinear effects to avoid parasitic phenomena like Brillouin and Raman scattering, which would impair laser performance. The reduction of nonlinear effects can be achieved using materials with reduced nonlinear properties, enhancing the mode area, or using shorter fiber lengths. The latter requires a distinct increase in RE concentration to maintain sufficient pump absorption.

The most common preparation technique for RE-doped fibers is the solution-doping method in combination with MCVD. The achievable dopant concentrations and core sizes are limited by the technology itself. In pure silica, the ytterbium solubility is limited to a few tens of mol ppm of Yb_2O_3.[16] By adding alumina in a molar ratio of $Al_2O_3/Yb_2O_3 > 4$, this limit can be extended to about 6000 mol ppm with a moderate optical background loss of < 100 dB/km.[17]

In recent years, a few alternative technologies have been developed to achieve larger active cores, higher RE concentrations, and homogeneous dopant profiles. One such technology is powder sinter material technology (REPUSIL), which has been demonstrated to fabricate fibers suitable for highly efficient high power fiber lasers.[22] Techniques based on the sintering of silica granulates[18,19] or on the sol–gel process[20,21] have also been established for making passive as well as active optical fibers. Another approach is the use of MCG glasses (e.g., SiO_2-Al_2O_3-La_2O_3 glass), a report on which is available in.[23] SiO_2-Al_2O_3-La_2O_3 (SAL) glasses with a high fraction of aluminum enable a very good solubility for RE ions. It is known[24] that high densities of excited ytterbium (Yb) ions enhance the photodarkening effect. The SAL glass system has the potential for high Yb concentration and low photodarkening because of the high amount of aluminum which can be incorporated. High aluminum concentration prevents the RE ions from clustering,[25] which is assumed to be a source of photodarkening.

Both nonlinear and fiber laser applications require fibers with a core-cladding structure. Such fibers can be made by combining an MCG core with a silica cladding. The latter method yields fibers with an enhanced mechanical stability and an extremely high numerical aperture. However, the typical thermochemical characteristics of MCGs, such as their relatively low melting temperature and their high thermal expansion coefficients, compared with silica glass, make the combination of MCG and fused silica a big challenge. One approach to span the thermal gap is to substitute volatile and thermal dissociative oxide components (e.g., lead oxide, antimony oxide, bismuth oxide) with lanthanum oxide. In the SAL glass system,[26] adapting to the thermal process parameters of silica is possible due to the high silicate concentration and the absence of alkaline ions or other extremely viscosity-depressing components.

In the present article, we will describe the preparation and characterization of SAL glass with high lanthanum and aluminum concentrations and the partial substitution of lanthanum with ytterbium. We have studied the effects of lanthanum and ytterbium in a wide range of concentrations on glass stability and on the thermal and optical properties of glass bulks as well as of unstructured and structured fibers. We will demonstrate the fabrication of fibers with passive and active SAL core glasses and their application for supercontinuum generation and ytterbium fiber laser operation, respectively.

Experimental Work

Glass Preparation and Characterization

Based on the starting composition of 70 mol% SiO_2, 20 mol% Al_2O_3, and 10 mol% La_2O_3, different glasses containing up to 24 mol% lanthanum oxide and up to 6 mol% ytterbium oxide were prepared in 500 g batches using a modified melting process. Relatively high amounts of Al_2O_3 (15–21 mol%) were added to increase the solubility of lanthanum and ytterbium in this high silica glass. Oxides (SiO_2, La_2O_3, Yb_2O_3, CeO_2) and hydroxide ($Al(OH)_3$) of high quality (3N–5N) were used as raw materials. The precursor

powder was thoroughly mixed and homogenized as well as directly sintered and melted in a covered platinum crucible in air atmosphere at temperatures between 1400 and 1650°C. Glass samples were prepared in a two-step discontinuous melting process to improve glass homogeneity. In the first melting step, the liquid melt was quenched in ultra-pure water to obtain fritted glass particles from 1 to 10 mm in size. In the second step, we re-melted the fritted and dried glass particles at 1650°C and partly stirred the melt for 4 h using a platinum stirrer to avoid striae and bubbles. We cast the liquid melt in a heat-resistant stainless steel mold to make glass blocks at a size of about 25 × 25 × 120 mm. Afterwards, the glass blocks were slowly cooled in a furnace starting from transition temperature (T_g) and going down to room temperature in about 1 day to reduce and avoid stress in the bulk glass.

The blocks were polished to inspect the homogeneity of the glass (striae, bubbles, and inclusions). Thermal properties, such as the glass transition temperature (T_g), dilatometric softening point (T_s), and thermal expansion coefficient (α @ 600°C), were measured with a vertical dilatometer (LINSEIS L75V) on glass bars (4 × 4 × 20 mm) using a heating rate of about 5 K/min. The absorption of polished glass slices with a thickness between 0.2 and 1 mm was studied using optical spectroscopy in the UV, Vis, and NIR region (190–2400 nm) using a Lambda 900 spectrometer (Perkin Elmer, Shelton, CT). All measurements were made using air as a reference. The refractive index n was determined at wavelengths of 633 and 1300 nm using a Prism Coupler Model 2010 (Metricon Corporation, Pennington, NJ) with an accuracy of about 10^{-3}. The glass composition was ascertained by quantitative electron probe microanalysis (EPMA) using energy dispersive X-ray analysis (EDX, JEOL JXA-8800L). The molar fractions were determined within a relative deviation of ± 5% related to the expected glass composition. To enhance the detection limit, wavelength dispersive measurements (WDX) were also carried out. This was performed especially in the case of samples with lower dopant levels. Table I and Table II list the measured compositions of SiO_2-Al_2O_3-La_2O_3 (SAL) glasses and Yb-doped SiO_2-Al_2O_3-La_2O_3 (SAL-Yb) glasses studied in this work.

Fluorescence properties, such as spectral behavior and the lifetime of the upper Yb^{3+} energy level, were measured on Yb-doped samples. A Ti sapphire laser at 880 nm (Lexel) and a MOPA system (SDL) at 976 nm were used as pump sources. The Yb^{3+} fluorescence was collected with the help of a 400 μm SiO_2 fiber and then guided to either an Instrument Systems fiber spectrometer to detect the spectral shape or to an oscilloscope with an InGaAs diode to detect the fluorescence decay.

Table I. Measured Glass Compositions of Lanthanum Aluminum Silicate (SAL) Glasses

	Glass sample					
mol%	1	2	3	4	5	6
SiO_2	69.6	64.9	64.4	60.1	60.5	55.7
Al_2O_3	20.8	20.8	16.4	21.2	15.5	20.2
La_2O_3	9.6	14.3	19.2	18.7	24.0	24.1

Fiber Fabrication and Characterization

Unstructured fibers made from uniform SAL glass blocks that have been ground and polished to cylindrical preforms with a diameter of about 18 mm and a length of 100 mm were used in the study of material-based spectral fiber loss. The surface of the glass cylinders was polished to improve the surface smoothness and to minimize surface-scattering losses. Then, they were drawn to fibers with a diameter of about 125 μm. Finally, they were coated with a single layer of high index acrylate (n = 1.51). Structured fibers with an outer diameter of about 125 μm and a core diameter of about 10 μm were prepared during the fiber-drawing process using a rod-in-tube (RIT) technique. In applications in which light is guided only in the core of the fiber (such as in supercontinuum generation), an acrylate coating (n = 1.51) was used to protect the fiber. For fiber laser tests, however, a fluorinated acrylate coating (n = 1.37) was used to enable cladding pumping. SAL/SiO_2 fibers and all-SAL (SAL core and SAL cladding) fibers were fabricated. The SAL core rods were prepared by stretching glass cylinders to an outer diameter of approximately 1 and 4 mm. As cladding tubes, fused high-purity silica tubes (Heraeus, Suprasil F300) with an inner diameter of 1 mm and an outer diameter of 15 mm or SAL tubes with an inner diameter of 4 mm, an outer diameter of about 20 mm, and a length of about 120 mm were used. One challenge to the fiber-drawing process is the difference in transition temperature and thermal expansion coefficient between the core and cladding material, particularly for the

Table II. Measured Glass Compositions of Yb-Doped Lanthanum Aluminum Silicate (SAL-Yb) Glasses

	Glass sample										
mol%	7	8	9	10	11	12	13	14	15	16	17
SiO_2	69.6	69.5	69.4	67.2	66.2	66.3	69.6	67.3	67.4	69.1	66.3
Al_2O_3	20.9	20.9	21.0	22.3	22.8	22.8	20.9	22.3	22.0	21.3	21.1
La_2O_3	9.4	9.3	9.0	9.7	9.9	8.9	6.2	6.2	5.2	3.6	11.0
Yb_2O_3	0.1	0.3	0.6	0.6	1.1	2.0	3.3	4.2	5.4	6.0	0.6
CeO_2				0.2							

combination of SAL/SiO_2. Adjustment of the drawing parameters, such as temperature, drawing force, preform feed rate, drawing speed, was extremely important in this process.

In all fibers, the attenuation $\beta(\lambda)$ was determined using the well-established cut-back method. The intensity transmitted in a longer piece of the fiber $I_1(\lambda)$ and a shorter piece of the fiber $I_2(\lambda)$ was measured using a fiber spectrometer (SPECTRO 320D from Instrument Systems, Munich, Germany and MS 9030A from Anritsu, Munich, Germany) and then compared logarithmically:

$$\beta(\lambda) = \frac{10 \cdot log \cdot \left(\frac{I2(\lambda)}{I1(\lambda)}\right)}{\Delta I}.$$

The fluorescence properties of Yb-doped fiber samples were also studied using the same setup and components as for the measurement of Yb-doped bulk samples.

Studies of photodarkening on Yb-doped SAL fibers were performed on step-index fibers with a core diameter of about 10 μm, a cladding diameter of 125 μm, and a fiber length of 1 cm (without coating). The test fibers were darkened by core pumping at 976 nm (Yb inversion about 0.46). For the temporal measurements of photodarkening loss, the transmission of probe light at 633 nm was analyzed with a lock-in amplifier technique. The experimental setup is described in more detail in.[27]

Studies have been performed to obtain low-loss splices between a SAL/SiO_2 fiber and a standard SiO_2 fiber (SMF28). Splice tests were performed using a BICC AFS 3100 splicing device.

Results and Discussion

SAL and SAL-Yb Bulk Glasses

Based on the Y_2O_3-Al_2O_3-SiO_2 ternary glass system reported by Hyatt, Day, and Shelby,[28,29] we replaced yttrium with the very similar lanthanum in order to increase the nonlinear properties and to match the thermochemical properties as much as possible to those of SiO_2. This is necessary for all aspects in which SAL glasses should be combined with SiO_2. Additionally, we partially substituted lanthanum with ytterbium as an active dopant. The glass forming region and glass stability of the lanthanum aluminum silicate system were studied concerning the La_2O_3/Yb_2O_3 concentration limits. Samples with 20 mol% Al_2O_3 and La_2O_3 concentrations between 10 and 24 mol% were made without phase separation and crystallization. These glasses were homogeneous and optically transparent after casting, and evaporation effects could not be observed at melting temperature. Glasses with 24 mol% La_2O_3 and 15 mol% Al_2O_3 showed an increased crystallization tendency after fine cooling (sample 5) or during the fiber-drawing process (samples 3 and 6). Hence, these glass compositions are not suitable for fiber fabrication.

The measured refractive indices and thermal properties of prepared lanthanum aluminum silicate glasses compared with commercial silica glass (Suprasil F300) are shown in Table III.

All-SAL glass compositions tested show a clearly higher transition temperature ($T_g \geq 860°C$) than commercially available heavy metal oxide glasses (e.g., flint glasses with $T_g = 719°C$, [31]). This is a great thermochemical advantage of SAL glasses with regard to their combination with undoped SiO_2 glass.

SAL glasses show a strong increase in refractive index compared with pure silica glass. Therefore, the total difference between their refractive index and the refractive index of pure silica (Δn) is assumed by the additive effects of lanthanum oxide (ΔnLa_2O_3) and aluminum oxide (ΔnAl_2O_3) corresponding to the following equation:

$$\Delta n = \Delta n_{La_2O_3} + \Delta n_{Al_2O_3}$$

Table III. Refractive Index and Thermal Properties of SAL Glasses Compared with Commercial Pure Silica Glass (Heraeus, Suprasil F300)

	Glass sample*						Silica
	1	2	3	4	5	6	F300
n@633 nm	1.601	1.651	1.695	1.693	1.736	1.740	1.456
n@1300 nm	1.590	1.638	1.681	1.678	1.720	1.723	1.447
Tg [°C]	870	861	861	861	875	868	1120[30]
Ts [°C]	929	922	916	917	927	924	
α [10^{-6}/K]	4.3	5.3	6.3	5.9	7.0	7.0	0.5

*The glass compositions are presented in Table I.

Based on the results presented in Table III, the refractive index increments relative to silica were estimated to be:

$$\Delta n_{La_2O_3} = +0.94 \cdot x_{La_2O_3}$$

$$\Delta n_{Al_2O_3} = +0.32 \cdot x_{Al_2O_3}$$

$x_{La_2O_3}$ and $x_{Al_2O_3}$ are the molar fractions of aluminum oxide and lanthanum oxide. The relative standard deviation for the measurement of Δn using the prism-coupling method is about 10%. Figure 1 shows the influence of aluminum and lanthanum oxide concentrations on the refractive index difference.[32,33] Glass sample 1, which contains 9.6 mol% La_2O_3, and a pure silica (F300) sample were studied using an absolute Z-scan measurement[34] to determine the nonlinear coefficient n_2. The absolute value of n_2 of the SAL glass was measured to be approximately two times larger than that of pure silica glass.

To extend the glass system for active fiber applications, we replaced La_2O_3 with Yb_2O_3. The effect of ytterbium oxide on thermal and optical glass properties was studied and is illustrated in Table IV. The increasing substitution of lanthanum with ytterbium leads to a decrease in refractive index and the thermal expansion coefficient, whereas the transition temperature increases slightly. Investigating ternary aluminum silicate glass systems with different RE ions, Kohli and Shelby[35] found out that the region of glass formation decreases if the radius of the incorporated RE ion decreases (ion radius: $Yb^{3+} < La^{3+}$). This could explain our experience with Yb-doped SAL glasses, namely: high doping levels of ytterbium ($\geq$ 10 mol% Yb_2O_3) proved critical with respect to crystallization and phase separation, whereas

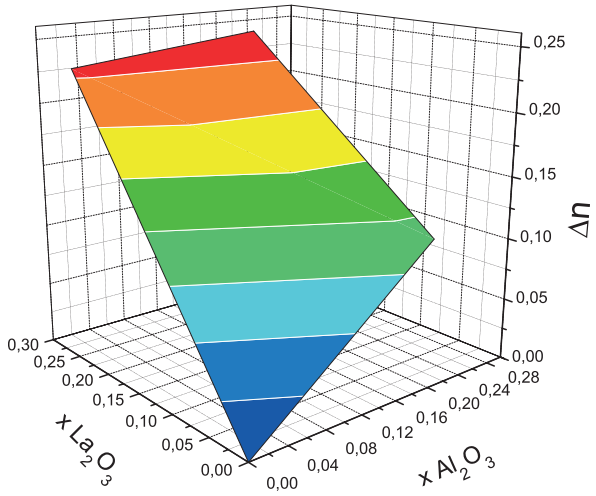

Fig. 1. Influence of the aluminum and lanthanum oxide concentrations on the refractive index difference compared with pure silica.

La_2O_3 could be incorporated into the same glass up to 24 mol% without a problem.

The absorption spectra of SAL glasses with different La_2O_3 contents are depicted in Fig. 2. SAL glasses have a transmission window between 250 and 2700 nm with a slight effect of the lanthanum content on the UV absorption edge (Fig. 2, inside). In Fig. 3a, the Yb^{3+} typical absorption spectra of the SAL-Yb glasses (Table II) are shown, and Fig. 3b manifests that at up to 6 mol% Yb_2O_3, no concentration quenching of the absorption coefficient is to be seen. At a value of about $2.5*10^{-24}m^2$ at 976 nm, both the spectral shape and the absorption cross-section of Yb^{3+} in SAL glasses are very similar to those known from Yb^{3+} in Al_2O_3/SiO_2 glasses made by MCVD.[36] On all-SAL-Yb glasses

Table IV. Refractive Index and Thermal Properties of SAL-Yb Glasses

	Glass sample*										
	7	8	9	10	11	12	13	14	15	16	17
n@633 nm	1.602	1.603	1.604	1.604	1.611	1.607	1.598	1.598	1.597	1.595	1.614
n@1300 nm	1.590	1.591	1.590	1.590	1.599	1.594	1.584	1.585	1.584	1.582	1.600
Tg [°C]	876	875	874	867	880	884	879	884	882	884	869
Ts [°C]	933	930	939	930	925	926	939	945	947	951	932
α [10^{-6}/K]	4.2	4.2	4.3	4.3	4.2	4.0	4.0	4.1	4.0	4.1	4.6

*The glass compositions are presented in Table II.

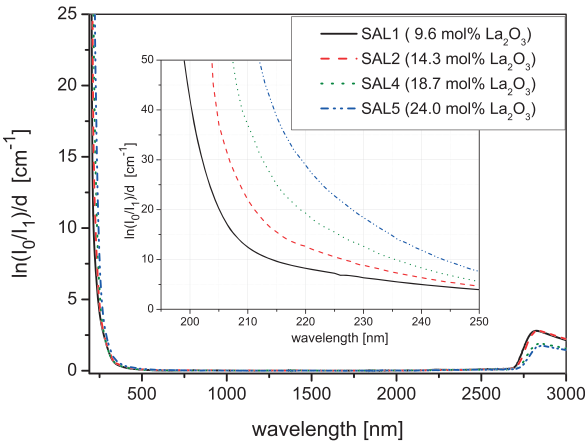

Fig. 2. Absorption spectra of Lanthanum aluminum silicate glasses with different La_2O_3 contents.

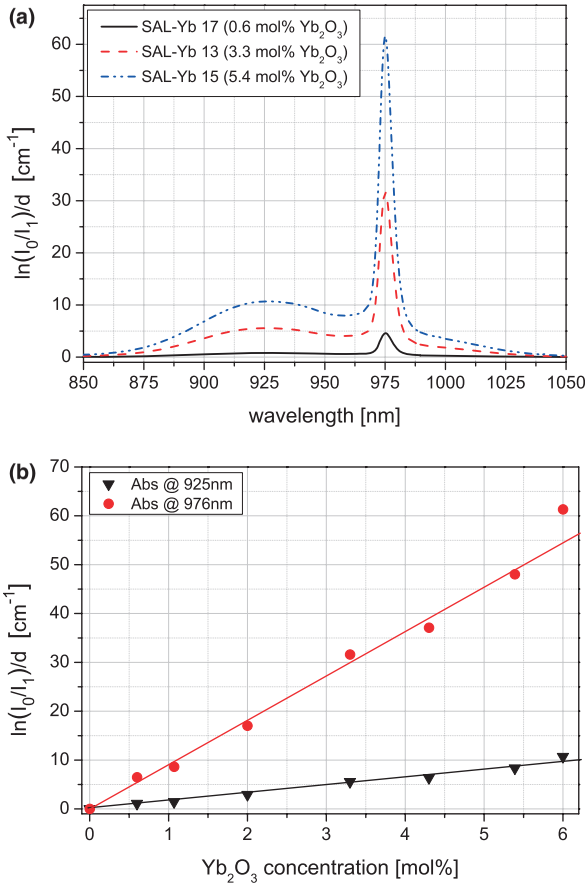

Fig. 3. (a) Absorption spectra of Yb^{3+} ion in the lanthanum aluminum silicate glass matrix with different Yb_2O_3 contents. (b) Absorption coefficients for Yb^{3+} ion at 976 nm and 925 nm.

summarized in Table II, the lifetime of the upper energy level of Yb^{3+} was measured. Despite the high Al_2O_3 and La_2O_3 content, the Yb^{3+} lifetime was found to be around 800 μs for Yb_2O_3 concentrations up to 0.6 mol% and then to decrease strikingly as the Yb content increased (Fig. 4). This behavior was found to be very similar to that of Yb^{3+} in SiO_2-based MCVD samples. Fluorescence measurements, especially those in the strongly ytterbium-doped bulk samples, often suffer from reabsorption effects, which can distort the spectral shape and lifetime. This can be averted using striping pump light incidence to involve only a very small sample volume in the measurement.

Unstructured Optical Fibers

Almost all-SAL bulk samples (with and without ytterbium) were prepared as polished cylinders and drawn into unstructured fibers for spectral loss characterization of the glass material. Background loss was caused by physical processes, such as absorption due to impurities (e.g., doping and OH content), inhomogeneities (e.g., bubbles, microcracks, and inclusions), and scattering. SAL core glasses with high La_2O_3 content (24 mol%) and low Al_2O_3 content (15 mol%) showed the onset of crystallization during the fiber-drawing process. In Fig. 5, typical loss spectra of unstructured fibers with SAL and SAL-Yb glass are depicted. The long interaction length of fibers makes it possible to identify even very small amounts of impurities based on their specific absorption bands. The first fiber exhibited broad absorptions between 600 and 1000 nm and peaked at 800 nm (fiber 1, SAL glass), which was probably caused by transition metal impurities (e.g., vanadium[37]) of the raw materials used. By changing the raw materials, these impurities could be minimized (fiber 2, SAL glass) and, finally, mostly eliminated (fiber 3, SAL-Yb glass). Then background losses with a value of 0.5 dB/m could be achieved even for Yb-doped SAL fibers (fiber 3). At a value of up to 3 dB/m, the OH absorption in the SAL fibers is rather high. Its location at 1417 nm is clearly red shifted compared with OH in pure silica glasses (1382 nm); this can be caused by the effect of the lanthanum ions on the glass network in the silica matrix. Fluorescence measurements were also performed on some unstructured Yb-doped fibers. The results do not differ from those made on bulk samples.

Structured Optical Fibers

All nonlinear or laser applications require fibers with a core-cladding structure. Such fibers can be produced in an all-SAL configuration (meaning that the core and cladding are both (all) made from SAL glasses) or in a configuration where the fiber combines an SAL core with a common fused silica cladding. The achievable refractive index of SAL glasses, which are stable enough to draw fibers, ranges from 1.60 to 1.65. This makes all-SAL step-index fibers with a numerical aperture of up to 0.4 possible. All-SAL fibers can be

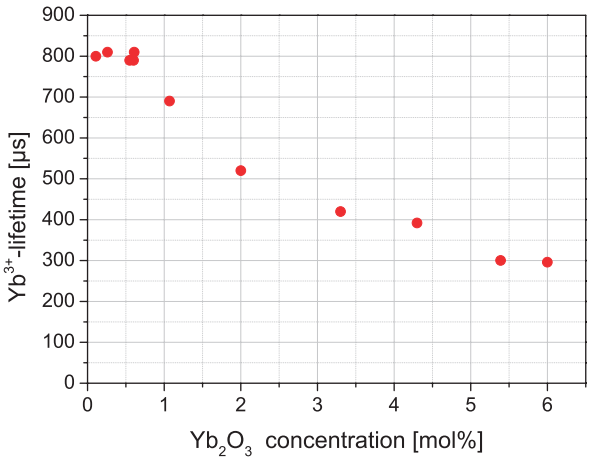

Fig. 4. Yb^{3+} lifetime of SAL-Yb bulk samples (summarized in Table II) depending on Yb_2O_3 content.

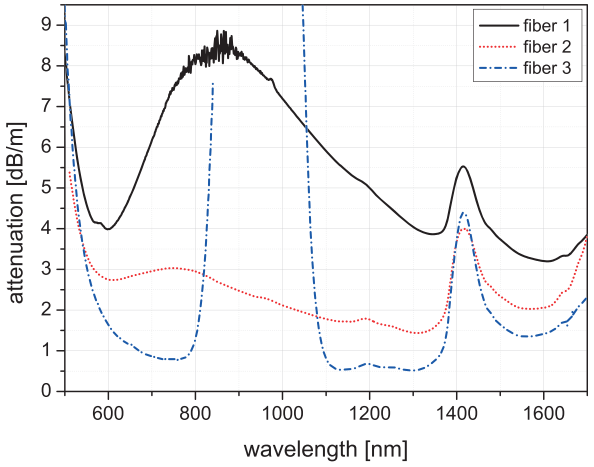

Fig. 5. Loss spectra of unstructured fibers with SAL (fiber 1 and 2) and SAL-Yb (fiber 3) glass prepared from raw materials with different purities.

drawn at around 1100°C due to their low glass transition temperature ($T_g \geq 860$°C). Unfortunately, the mechanical stability of such fibers is much lower than that of SiO_2 fibers. By combining SAL as a core glass with a SiO_2 cladding, a refractive index difference between the core and cladding of up to 0.2 can be achieved. In such fibers, numerical apertures of up to 0.8 are attainable. Additionally, the mechanical stability —and thus the handling—is similar to SiO_2 fibers. Nevertheless, fabricating such combined SAL/SiO_2 fibers presents a major technological challenge due to the clearly different thermochemical properties of both glasses. The viscosity gap between the SAL core glass and the silica cladding is larger than four orders of magnitude at a fiber-drawing temperature of 1850°C. This was discussed in detail in.[38] Depending on the core glass composition, the drawing conditions (the preform feed rate and the necessary drawing speed in particular) were adjusted accordingly to avoid, for example, the enlarging of the core that is often observed. Losses measured on combined fibers are similar to those of unstructured fibers (Fig. 6).

Passive Optical Fibers for Nonlinear Applications

A promising application of nonlinear behavior of structured SAL fibers is white light emission by supercontinuum generation. A step-index fiber with an outer diameter of 210 µm and an SAL core glass (sample 1) with a diameter of 3.5 µm was tested in a supercontinuum generation setup. The core diameter was selected to blue shift the zero dispersion wavelength (ZDW) of the fundamental mode below the laser wavelength in order to generate nonlinear effects in the anomalous dispersion regime. At nearly 1447 nm, the ZDW of the fundamental mode was clearly shifted to a higher wavelength compared with silica and close to the pump wavelength (Fig. 7). The dispersion was measured interferometrically. The fiber was pumped with a femtosecond laser at a wavelength of 1550 nm at a repetition rate of 110 MHz and a peak power of about 23 kW (mean power of 200 mW). The supercontinuum was obtained by generating solitons and phase-matched radiations (and other nonlinear effects) through a 3-m-long piece of fiber. Figure 8 shows the spectral development of the emission band. The supercontinuum changes at the blue edge from a wavelength of 1.4 to 1.0 µm with an increase in pump power. For the highest available power, emissions range from 1.0 µm to at least 1.7 µm. Development in the wavelength range above 1.7 µm could not be measured due to the limited detection window of the optical spectrum analyzer. Broadening above the 2 µm range can be expected.

Active Optical Fibers for Laser Applications

The measured Yb^{3+} lifetime of prepared structured fibers is comparable with the values of unstructured fibers and the corresponding bulk glass material

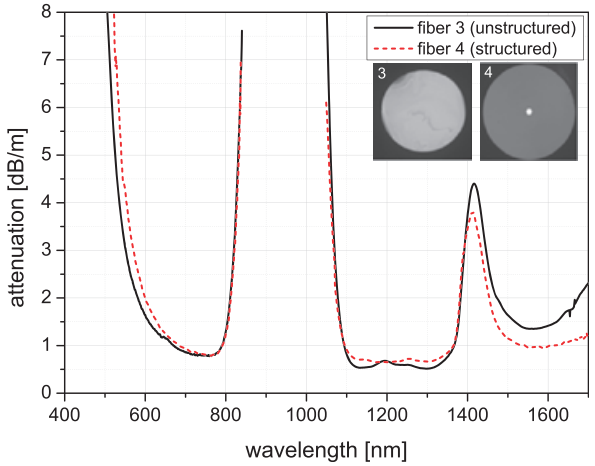

Fig. 6. Loss spectra of an unstructured (fiber 3) and a structured (fiber 4) fiber of the same Yb-doped core glass (SAL-Yb 10) with silica cladding.

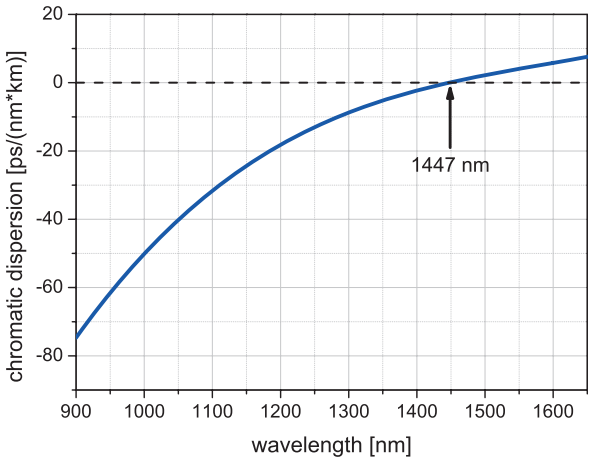

Fig. 7. Chromatic dispersion measurement on step-index fiber with SAL core glass.

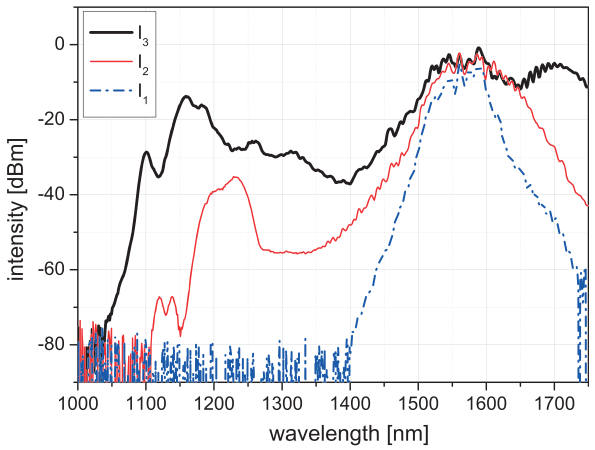

Fig. 8. Supercontinuum generation in a fiber with SAL core glass pumped at 1550 nm (pump power increases from I_1 to I_3).

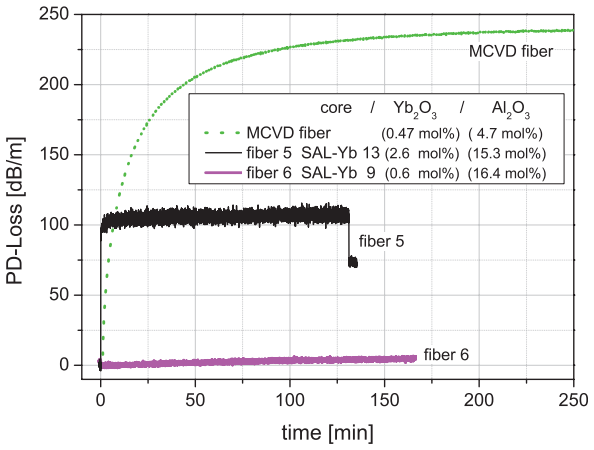

Fig. 9. Temporal course of the PD loss at a probe wavelength of 633 nm measured during core pumping with 976 nm (Yb inversion 0.46) on SAL/SiO_2 fibers with different ytterbium concentration and comparison with an Yb-doped fiber made by MCVD.

(Fig. 4). The long-term stability of the active fiber during the laser process is very important and may be limited, for example, by the photodarkening (PD) of the fiber used. The PD effect is stronger the higher the Yb_2O_3 concentration is and can lead to a systematic reduction in laser efficiency.[39]

Photodarkening was studied on step-index fibers with different SAL-Yb core glasses. The decrease in fiber transmittance was measured during core pumping of short fiber pieces (length: 1 cm) with a pump wavelength of 976 nm to accelerate the degradation process and to determine the PD loss curves. Figure 9 shows the temporal course up to the equilibration of the PD loss for the different fibers. It was found that an SAL-Yb core glass fiber (fiber 6) exhibits a lower PD effect than an MCVD fiber with a similar Yb_2O_3 concentration. The reduced PD loss of the SAL glass fiber can be explained by the very high Al_2O_3 concentration of the core glass and is a known phenomenon in Yb laser fibers.[21] However, the PD process is much faster in the case of high Yb concentration (fiber 5), and remarkable loss is observed. An additional effect of La_2O_3 concentration on PD is presumed, but there is no evidence yet to support this presumption. To analyze PD behavior in the existing setup, the fiber being tested is to be spliced between standard single-mode fibers with a Ge-doped silica core. This procedure is very challenging and time-consuming because of the different thermal properties of both core materials. Splice loss values below 1 dB can be achieved. If the pump power is switched on or off, an immediate change in fiber loss is observed that may be partly attributed to a thermal modification in splice loss due to Yb absorption. Further studies are required to improve the reliability of splices between fibers with silica and SAL glass cores.

Based on this research, the promising high Yb-doped SiO_2-Al_2O_3-La_2O_3 glass system was identified and found to be well suited for cw application. It is particularly well suited for pulsed, high power fiber laser operation at enhanced Yb inversion. For the first laser experiments, we selected fibers with different core-cladding composite structures. We chose one fiber with an SAL core glass and a pure silica cladding (fiber 7) to achieve high core numerical apertures; however, we also chose one fiber with an SAL-Yb glass core and an SAL glass cladding (fiber 8) to achieve low core numerical apertures. The fibers with an outer diameter of about 200 µm and a length of 60-80 cm were tested in a Fabry Perot laser setup in continuous operation similar to the one described in.[18] The fiber is pumped by a 200 µm fiber-coupled diode laser at 915 nm. The pump light is absorbed in the fiber core and converted into higher beam quality laser light in the wavelength range from 1050 to 1090 nm as depicted in Fig. 10 (inset). Figure 10 shows the measured laser characteristic of the different fibers. In the power range of up to 5 W, a laser efficiency of about 41% could be demonstrated with an Yb-doped fiber composed of an SAL glass core and SAL glass cladding (fiber 8). To enhance the laser efficiency of these novel types of Yb laser

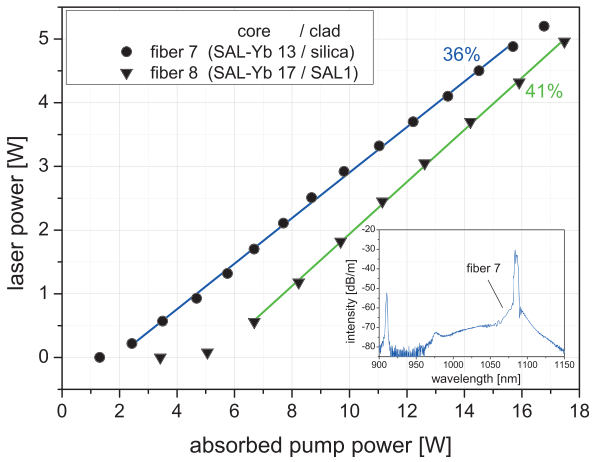

Fig. 10. Laser characteristics of step-index fibers with different core-cladding composite structures.

fibers, further studies are needed to reduce the loss of pump and laser power in the structured fibers and in the glass material, respectively.

Conclusion

Various SAL glasses were prepared using crucible melting technology. Their composition was changed in a wide range to optimize the thermochemical properties for fiber drawing and the optical properties for nonlinear and fiber laser applications. Due to the highly achievable rare earth amount of about 24 mol% La_2O_3 and 6 mol% Yb_2O_3, SAL glasses exhibit a high refractive index (1.6–1.74) and a nonlinear coefficient twice as high as that of SiO_2. Both the absorption and the lifetime of Yb-doped SAL glass hardly differ from Yb-doped silica. Despite a glass transition temperature of 860°C, step-index fibers with an SAL core and a silica cladding were drawn. Such fibers show advantageous properties, such as mechanical stability, improved nonlinear coefficient, and high ytterbium solubility. Fibers with background losses as low as 0.5 dB/m were developed and successfully used for supercontinuum generation between 1025 nm and at least 1750 nm. Fiber laser operation around 1080 nm was demonstrated at an efficiency of 41%. The photodarkening effect seems to be remarkably reduced in SAL-Yb glasses compared with MCVD silica fibers with similar Yb content. This is probably due to the high aluminum concentration achievable in crucible-melted SAL glasses. Thus, SAL glasses have a large potential for nonlinear and fiber laser applications.

Acknowledgments

The authors would like to thank the Thuringian Ministry of Economy, Employment, and Technology (TMWAT) and the European Regional Development Fund (EFRE) for their support within the framework of the "NEODIN" Project and the VORTEX Project—Limousin Region (EFRE). We wish to thank P. Dittmann and F. Lindner for their help in preparing glass melts, J. Bierlich, S. Fehling, T. Eschrich, A. Scheffel, Ch. Schmidt, and M. Arnz for technical support; and K. Fedus and G. Boudebs from the University of Angers, France, for the nonlinear characterization of glass.

References

1. H. Ebendorff-Heidepriem *et al.*, "Bismuth Glass Holey Fibers with High Nonlinearity," *Opt. Express*, 12 [21] 5082–5087 (2004).
2. X. Feng, A. K. Mairaj, D. W. Hewak, and T. M. Monro, "Nonsilica Glasses for Holey Fibers," *J. Lightwave Technol.*, 23 [6] 2046–2054 (2005).
3. Y. P. Yatsenko *et al.*, "Dispersion and Guidance Characteristics of Microstructured $68TeO_2 - 22WO_3 - 8La_2O_3 - 2Bi_2O_3$ Glass Fibres for Supercontinuum Generation," *Quantum Electron.*, 40 [6] 513–518 (2010).
4. M. N. Mohd Nasir, Z. Yusoff, M. H. Al-Mansoori, H. A. Abdul Rashid, and P. K. Choudhury, "On the Pre-Amplified Linear Cavity Multi-Wavelength Brillioun-Erbium Fiber Laser with Low SBS Threshold Highly Nonlinear Photonic Crystal Fiber," *Laser Phys.*, 19 [10] 2027–2030 (2009).
5. T. Sylvestre, A. Kudlinski, A. Mussot, J. F. Gleyze, A. Jolly, and H. Maillotte, "Parametric Amplification and Wavelength Conversion in the 1040–1090 nm Band by Use of a Photonic Crystal Fiber," *Appl. Phys. Lett.*, 94 (11) 111104-1–111104-3 (2009).
6. A. A. Voronin *et al.*, "Understanding the Nonlinear-Optical Response of a Liquid-Core Photonic-Crystal Fiber," *Laser Phys. Lett.*, 7 [1] 46–49 (2010).
7. P. Domachuk *et al.*, "Over 4000 nm Bandwidth of Mid-IR Supercontinuum Generation in sub-centimeter Segments of Highly Nonlinear Tellurite PCFs," *Opt. Express*, 16 [10] 7161–7168 (2008).
8. H. Garcia, A. M. Johnson, F. A. Oguama, and S. Trivedi, "New Approach to the Measurement of the Nonlinear Refractive Index of Short (<25m) Lengths of Silica and Erbium-Doped Fibers," *Opt. Lett.*, 28 [19] 1796–1798 (2003).
9. A. Mori *et al.*, "1.5μm band zero-dispersion shifted tellurite photonic crystal fibre with a nonlinear coefficient γ of $675W^{-1}km^{-1}$," 30th ECOC, paper Th3.3.6 (2004).
10. V. V. R. K. Kumar *et al.*, "Extruded Soft Glass Photonic Crystal Fiber for Ultrabroad Supercontinuum Generation," *Opt. Express*, 10 1520–1525 (2002).
11. F. G. Omenetto *et al.*, "Spectrally Smooth supercontinuum from 350 nm to 3 μm in Sub-Centimeter Lengths of Soft-Glass Photonic Crystal Fibers," *Opt. Express*, 14 4928–4934 (2006).
12. A. Labruyère *et al.*, "Structured-Core GeO_2-Doped Photonic-Crystal Fibers for Parametric and Supercontinuum Generation," *IEEE Photonics Technol. Lett.*, 22 [16] 1259–1262 (2010).
13. V. Tombelaine *et al.*, "Nonlinear Photonic Crystal Fiber with a Structured Multi-Component Glass Core for Fourwave Mixing and Supercontinuum Generation," *Opt. Express*, 17 [18] 15392–15401 (2009).

14. A. Boucon *et al.*, "Supercontinuum Generation From 1.35 to 1.7 μm by Nanosecond Pumping Near the Second Zero-Dispersion Wavelength of a Microstructured Fiber," *IEEE Photonics Technol. Lett.*, 20 [10] 842–844 (2008).
15. W. Q. Zhang, H. Ebendorff-Heidepriem, T. M. Monro, and V. S. Afshar, "Fabrication and Supercontinuum Generation in Dispersion Flattened Bismuth Microstructured Optical Fiber," *Opt. Express*, 19 [22] 21135–21144 (2011).
16. P. Barua, E. H. Sekiya, K. Saito, and A. J. Ikushima, "Influences of Yb3 + ion Concentration on the Spectroscopic Properties of Silica Glass," *J. Non-Cryst. Solids*, 354 4760–4764 (2008).
17. J. Kirchhof, S. Unger, and A. Schwuchow, "Properties of Yb-doped materials for solid and microstructured high power fiber lasers," Proceedings of ICMAT 2007 Symposium on Microstructured and Nanostructured Optical Fibers, Singapore, July 1-6, 2007.
18. L. di Labio, W. Lüthy, V. Romano, F. Sandoz, and T. Feurer, "Broadband Emission from a Multicore Fiber Fabricated with Granulated Oxides," *Appl. Opt.*, 47 [10] 1581–1584 (2008).
19. R. Renner-Erny, L. di Labio, and W. Lüthy, "Novel Technique for Active Fibre Production," *Opt. Mater.*, 29 [8] 919–922 (2007).
20. V. Matejec, M. Hayer, M. Pospisililova, and I. Kasik, "Preparation of Optical Cores of Silica Optical Fibers by the Sol-Gel Method," *J. Sol-Gel. Sci. Technol.*, 8 889–893 (1997).
21. M. Locher, D. Michel, W. Luthy, and H. P. Weber, "Rare-Earth Doped Sol-Gel Materials for Optical Waveguides," *Opt. Lasers Eng.*, 43 [3-5] 341–347 (2005).
22. M. Leich *et al.*, "Highly Efficient Yb-Doped Silica Fibers Prepared by Powder Sinter Technology," *Opt. Lett.*, 36 1557–1559 (2011).
23. M. J. Dejneka *et al.*, "La_2O_3-Al_2O_3-SiO_2 Glasses for High-Power, Yb^{3+}-Doped, 980-nm Fiber Lasers," *J. Am. Ceram. Soc.*, 85 [5] 1100–1106 (2002).
24. S. Jetschke, S. Unger, U. Röpke, and J. Kirchhof, "Photodarkening in Yb Doped Fibers: Experimental Evidence of Equilibrium States Depending on the Pump Power," *Opt. Express*, 15 14838–14843 (2007).
25. S. Jetschke, S. Unger, A. Schwuchow, M. Leich, and J. Kirchhof, "Efficient Yb Laser Fibers with Low Photodarkening by Optimization of the Core Composition," *Opt. Express*, 16 15540–15545 (2008).
26. S. Iftekhar, J. Grins, and M. Eden, "Composition-Property Relationships of the La_2O_3-Al_2O_3-SiO_2 Glass System," *J. Non-Cryst. Solids*, 356 1043–1048 (2010).
27. M. Leich, U. Röpke, S. Jetschke, S. Unger, V. Reichel, and J. Kirchhof, "Non-Isothermal Bleaching of Photodarkened Yb–Doped Fibers," *Opt. Express*, 17 12588–12593 (2009).
28. M. J. Hyatt, and D. E. Day, "Glass Properties in the Yttria-Alumina-Silica-System," *J. Am. Ceram. Soc.*, 70 [10] C283–C287 (1987).
29. J. E. Shelby, *Rare Elements in Glasses, Key Engineering Materials*, Vol. 94-95, Trans Tech Publications, Switzerland, 1994.
30. J. Kirchhof, and A. Funke, "Reactor Problems in Modified Chemical Vapour Deposition (II) – The mean Viscosity of Quartz Glass Reactor Tubes," *Cryst. Res. Technol.*, 21 [6] 763–770 (1986).
31. Available at SCHOTT Optical Glass Catalog http://www.us.schott.com/advanced_optics/english/our_products/materials/data_tools/index.html (accessed September 6, 2012).
32. J. Kobelke *et al.*, "Fabrication and Characterization of Special Microstructured Fibers," Proceedings of SPIE Europe, Prague, 8001–8 (2011).
33. K. Schuster *et al.*, "Structured material combined HMO-Silica Fibers – preparation, optical and mechanical behavior," Proceedings of SPIE, Photonics West, San Francisco, 7934–24 (2011).
34. G. Boudebs, and K. Fedus, "Absolute Measurement of the Nonlinear Refractive Indices of Reference Materials," *J. Appl. Phys.*, 105 103–106 (2009).
35. J. T. Kohli, and J. E. Shelby, "Formation and Properties of Rare-Earth Aluminosilicate Glasses," *Phys. Chem. Glasses*, 32 [2] 67–71 (1991).
36. M. A. Melkumov, I. A. Bufetov, K. S. Kravtsov, A. V. Shubin, and E. M. Dianov, "Lasing Parameters of Ytterbium-Doped Fibres Doped with P_2O_5 and Al_2O_3," *Quant. Electr.*, 34 [9] 843–848 (2004).
37. P. C. Schultz, "Optical Absorption of the Transition Elements in Vitreous Silica," *J. Am. Ceram. Soc.*, 57 [7] 309–313 (1974).
38. J. Kobelke *et al.*, "Highly Germanium and Lanthanum Modified Silica Based Glasses in Microstructured Optical Fibers for Non-Linear Applications," *Opt. Mater.*, 32 1002–1006 (2010).
39. I. Manek-Hönninger *et al.*, "Photodarkening and Photobleaching of an Ytterbium-Doped Silica Double-Clad LMA Fiber," *Opt. Express*, 15 1606–1611 (2007).